Chem Soc Rev

Cite this: *Chem. Soc. Rev.*, 2012, **41**, 52–67

www.rsc.org/csr

TUTORIAL REVIEW

Recent progress in fluorescent and colorimetric chemosensors for detection of amino acids

Ying Zhou[ab] and Juyoung Yoon*[a]

Received 10th June 2011
DOI: 10.1039/c1cs15159b

Due to the biological importance of amino acids, the development of optical probes for these molecules has been an active research area in recent years. This *tutorial review* focuses on recent contributions since the year 2000 concerning the fluorescent or colorimetric sensors for amino acids, and is organized according to their structural classification and reaction types. For reaction based chemosensors, the works are classified according to the mechanisms between sensors and amino acids, including imine formation, Michael addition, thiazinane or thiazolidine formation, cleavage of a sulfonate ester, cleavage of disulfide, metal complexes-displace coordination and others.

1. Introduction

Amino acids (AA), the key constituents of proteins, are small molecules with various functional side chain groups, which result in different roles of amino acids in physiological processes.[1] In this family, lysine (Lys) is closely related to the Krebs–Henseleit cycle and polyamine synthesis, and an appropriate amount of lysine in the diet is essential for the metabolic functions and weight gain of animals;[2] histidine (His) is essential for the growth and repair of tissue as well as for the control of metal elements transmission in biological bases;[3] tryptophan (Trp) plays a crucial part in biological processes such as protein biosynthesis, animal growth, and plant development.[4] In addition, the deficiency of some amino acids causes various abnormalities, for example, deficiency of cysteine (Cys) results in slow growth, hair depigmentation, edema, lethargy, liver damage, muscle and fat loss.[5]

As the result of increasing attention paid to human health, and diagnosis and treatment of disease, many efforts have been directed to the development of new methods toward amino acid analysis. Currently, the most used analytical procedures to detect and characterize amino acids are based on spectroscopic,[6] chromatographic[7] or electrochemical approaches.[8] However, each approach has some drawbacks such as the need of apparatus and trained personnel, operational convenience, analysis cost, test speed and detection

[a] *Department of Chemistry and Nano Science and Department of Bioinspired Science (WCU), Ewha Womans University, Seoul 120-750, Korea. E-mail: jyoon@ewha.ac.kr; Fax: +82-2-3277-2384; Tel: +82-2-3277-2400*
[b] *School of Chemical Science and Technology, Yunnan University, Kunming 650091, P. R. China*

Ying Zhou

Ying Zhou was born in Shenyang, China, in 1978. She received her PhD in 2008 from Dalian University of Technology under the supervision of Prof. Xuhong Qian. Subsequently she joined the group of Juyoung Yoon at Ewha Womans University as a postdoctoral fellow. In 2010, she became a staff member of Yunnan University. Her recent research focuses on the fluorescence chemosensors and the organic electroluminescent materials.

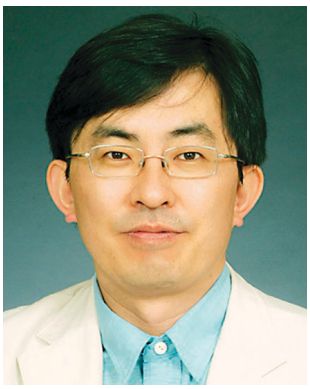

Juyoung Yoon

Juyoung Yoon was born in Pusan, Korea, in 1964. He received his PhD (1994) from The Ohio State University. After completing postdoctoral research at UCLA and at Scripps Research Institute, he joined the faculty at Silla University in 1998. In 2002, he moved to Ewha Womans University, where he is currently a Professor of Department of Chemistry and Nano Science and Department of Bioinspired Science. His research interests include investigations of fluorescent chemosensors, molecular recognition and organo EL materials.

limit, *etc*. Although there are numerous systems for their detection, there is still a need to develop novel and simple fluorescent and colorimetric chemosensors for visual discrimination due to their ease of use in solution as well as the high sensitivity and selectivity.[9] Therefore, the interest in developing optical chemosensors specifically recognizing a target amino acid has grown steadily, and the ability to easily and quickly obtain fingerprints for different amino acids by chemosensors will still constitute a breakthrough.

Recent advances in the field of amino acid sensing have focused on the use of fluorescent and colorimetric methods for the enantioselective discrimination of amino acids. Indicator-displacement assays, metal complexes coordination, specific reactions between probes and amino acids and other ways have been widely utilized. Since the chemosensors for Cys have been recently reviewed,[10] the very latest contributions for Cys selective chemosensors are included here. In this tutorial review, we focus on the fluorescent and colorimetric chemosensors developed since the year 2000 for the detection of basic amino acids. These sensors are classified according to their structural classifications. We hope to provide a general overview of the design and applications of these chemosensors for the detection of amino acids.

2. Fluorescent and colorimetric chemosensors for detecting amino acids

2.1 Fluorescent and colorimetric chemosensors based on metal complexes

2.1.1 Chemosensors based on copper complexes. In 2001, Klein and Reymond reported a copper complex of the quinacridone ligand **1** that operates as a fluorescent sensor for amino acids L-methionine (Met) and L-leucine (Leu) (Fig. 1).[11] The rapid ligand exchange kinetics of this sensor allowed it to follow the reaction of acylase and aminopeptidase, two enzymes that release free amino acids from non-coordinating precursors. Fluorescence increase of sensor **1** in the presence of Cu^{2+} ions upon simulated conversion of *N*-acetyl-L-methionine into L-methionine (in bis-tris (pH = 7.2), water/DMSO (60/40)) and L-leucinamide into L-leucine (in tris (pH = 9.0), water/DMF (60/40)) was observed at $\lambda_{em} = 580 \pm 50$ nm.

Reymond and co-workers further explored a water soluble fluorescein-based ligand **2** forming a non-fluorescent complex with Cu^{2+} (Fig. 2).[12] This complex served as a fluorescent

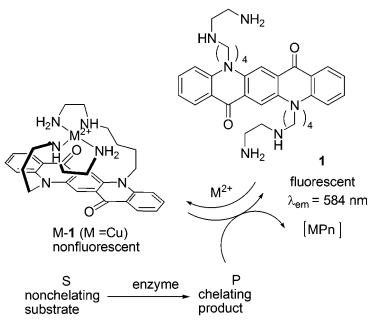

Fig. 1 Principle of the fluorescence enzyme assay using **1**.

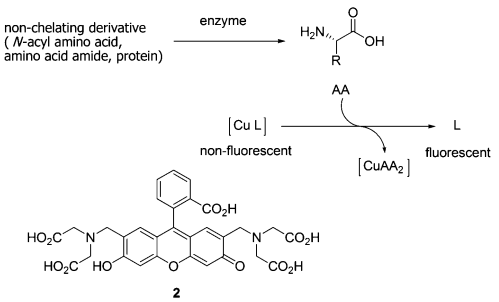

Fig. 2 Principle of a fluorescence assay for amino acids using copper-ligand complexes.

sensor for most amino acids in the 10^{-3} M concentration range. Cysteine resulted in a full return of fluorescence upon addition of one equivalent relative to Cu^{2+}. Since the signal response was very fast, the sensor can be used to detect the hydrolytic activity of various proteases (trypsin, chymotrypsin, subtilisin) on bovine serum albumin as a whole protein substrate, and more generally to follow reactions releasing or removing free amino acids in real time.

In 2003, Fabbrizzi *et al*. reported an *off–on* chemosensing ensemble for selective recognition of the ambidentate imidazole residue of histidine over the carboxylate group of natural amino acids *via* the indicator-displacement assays (IDAs) (Fig. 3).[13] Coumarine 343, fluorescein, and eosine Y were used as the indicators. Titration of each indicator with the $[Cu^{2+}_2(3)]^{4+}$ receptor complex at pH = 7 resulted in a complete quenching of the emission. The $[Cu^{2+}_2(3)]^{4+}$/coumarine ensemble does not discriminate His and glycine (Gly), while the fluorescein-containing ensemble satisfactorily discriminates His with full recovery of fluorescence from Gly. The highest sensing selectivity is observed with the $[Cu^{2+}_2(3)]^{4+}$/eosine Y ensemble. The observed trend of stability of other amino acids (Gly > alanine (Ala) > phenylalanine (Phe) > valine (Val) > Leu > proline (Pro)) seems to be related to the increasing steric repulsive effects exerted by the substituent.

In light of their previous work, Fabbrizzi and co-workers reported a dicopper(II) octamine cage as a selective receptor for L-glutamate ion in water at pH 7, establishing Cu^{2+}/–COO^- coordinative interactions (Fig. 4).[14] L-Glutamate (Glu) was able to displace the quenched rhodamine indicator (**7**) from the cage, whose fluorescence was then fully restored. Addition of **5** caused the fluorescence intensity of **7** to decrease, until complete quenching occurred. A 1 : 1 adduct between the dimetallic cage **5** and the indicator **7**, whose association constant log K_{ass} is 7.0 ± 0.2, was formed. The solution was titrated with a solution of L-glutamic acid. And, upon titration, fluorescence of **7** at 571 nm was progressively

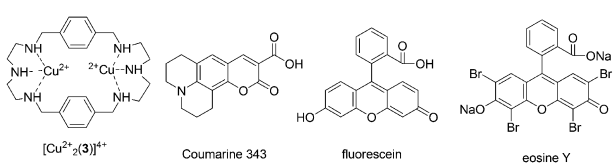

Fig. 3 The structures of $[Cu^{2+}_2(3)]^{4+}$, Coumarine 343, fluorescein, and eosine Y.

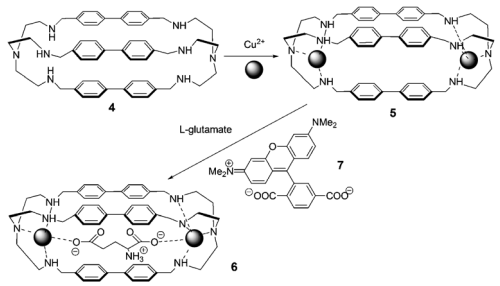

Fig. 4 Cascade mechanism for the consecutive inclusion of two Cu^{2+} ions and a dicarboxylate ion (*e.g.*, glutamate) within a bis-tren cage with diphenyl spacers.

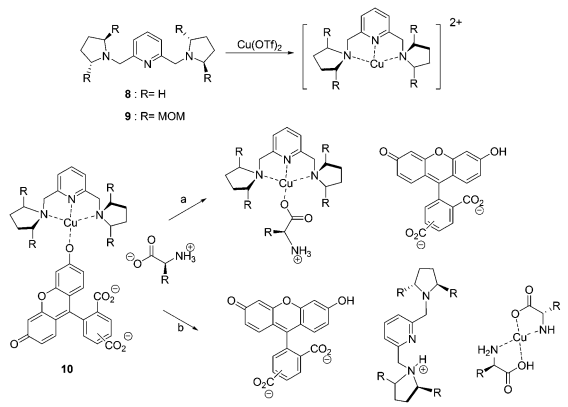

Fig. 5 The structures of **8**, **9** and two pathways for the displacement of indicator **10** from a Cu^{2+}-containing receptor by an L-amino acid guest.

restored. A value of log K_{ass} = 6.9 ± 0.2 was obtained for the adduct-formation equilibrium.

In 2005, coordinatively unsaturated metal complexes were reported by Anslyn *et al.* (Fig. 5).[15] The receptors **[Cu(8)]$^{2+}$** and **[Cu(9)]$^{2+}$** were found to discriminate His from other zwitterionic α-amino acids by means of IDAs using 5(6)-carboxyfluorescein as an indicator. The titrations of each of the complexes into solutions of the indicator caused an increase in the absorbance at 494 nm resulting in a visual color change from a bright yellow green to a dark yellow brown in buffered MeOH/H_2O (3 : 1) solution. The colorimetric detection of His was achieved by using this IDA method, which appears to owe its selectivity to a unique process involving disruption of the host complex to form a 2 : 1 His/Cu^{2+} complex rather than simple indicator displacement.

In the same year, Anslyn *et al.* reported another operationally simple sensing scheme based on competitive dynamic metal coordination (Fig. 6).[16] Pyrocatechol violet (PV) was used in this indicator displacement assay to effectively compete

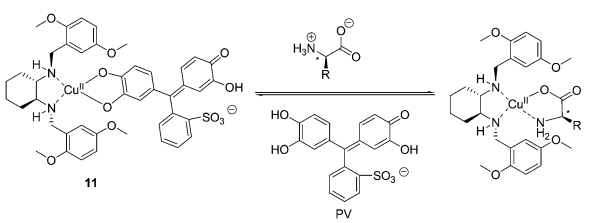

Fig. 6 The proposed binding mode of host **11**, indicator (PV) with amino acids.

with the amino acid guest for open coordination sites on **(*S*,*S*)-11–Cu^{2+}**. Titration of **(*S*,*S*)-11–Cu^{2+}** with PV gave a 1 : 1 complex with a shift from 445 to 645 nm, resulting in a change in color from pale yellow to intense blue. Addition of amino acid to the **(*S*,*S*)-11–Cu^{2+}**/PV complex resulted in the reversal of the spectral change, signaling PV displacement. Relationships between ee and absorbance were obtained in 1 : 1 MeOH/H_2O (50 mM HEPES buffer pH = 7.0). The resultant ee *versus* *A* relationships are remarkably linear (R^2 > 0.99), demonstrating uniform sensitivity over the entire ee range.

Anslyn and co-workers further reported the discrimination of enantiomeric and structurally similar amino acids through a series of IDAs based on dynamic metal coordination (Fig. 7).[17] The selected indicators, chromophores pyrocatechol violet (PCV), chromoxane cyanin R (CCR) and chrome azurole S (CAS), undergo large red shifts in their absorbance spectra upon Cu^{2+} coordination, thus providing a highly sensitive colorimetric output. The sense of enantioselectivity exhibited in each IDA was found to be a general property of the chiral receptor, with complexes **12**–Cu^{2+} and **13**–Cu^{2+} preferring L configurations while **14**–Cu^{2+} favoring D configurations. Because free CAS is yellow in color and Cu^{2+}-bound CAS is blue, the ratio of the bound to the free indicator, which depends on the stability of the receptor–amino acid complex, can be assessed by visual inspection (1 : 1 MeOH : H_2O, 50 mM HEPES buffer, pH = 7.8). All of the IDAs conformed to the relative chemoselective ordering for complex stability, as Trp > Phe > Leu ≈ Val > *tert*-leucine (Tle).

Anslyn *et al.* extended the scope of the previous study by an enantioselective indicator displacement assay (eIDA) (Fig. 8).[18]

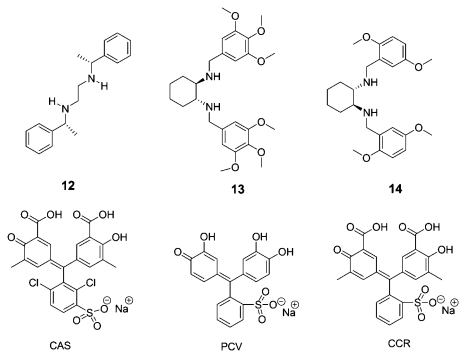

Fig. 7 The structures of compounds **12–14** and indicators (CAS, PCV, CCR).

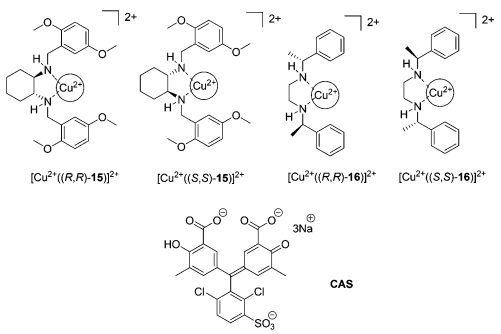

Fig. 8 The structures of copper complexes of **15–16** and indicators (CAS).

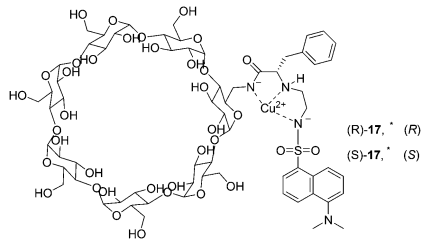

Fig. 9 Schematic structures of the Cu^{2+} complexes of dansylated cyclodextrins **(*R*)-17** and **(*S*)-17**.

One of the two chiral receptors (**[Cu^{2+}(15)]$^{2+}$** or **[Cu^{2+}(16)]$^{2+}$**) and chrome azurol S (CAS), as the indicator, were used to enantioselectively discriminate 13 α-amino acids in aqueous medium (1 : 1 MeOH : H_2O, HEPES pH = 7.5). **[Cu^{2+}((*R*,*R*)-15)]$^{2+}$** was generally found to bind more strongly to L-α-amino acids, however in the case of aspartate, asparagine, and histidine, the D-enantiomer was preferred by receptor **[Cu^{2+}((*R*,*R*)-15)]$^{2+}$**. Enantiomeric excess was determined for true test samples using ee calibration curves to demonstrate the capabilities of eIDAs.

In 2000, two modified cyclodextrins were described by Corradini and co-workers (Fig. 9).[19] Addition of D- or L-amino acids to the Cu^{2+} complexes induced a 'switch on' of the fluorescence. The complex **Cu–(*S*)-17** showed better discriminating properties than **Cu–(*R*)-17**. The best enantioselectivity was observed for Pro with both cyclodextrins, with reversed order ($\Delta F_D/\Delta F_L$ = 3.89 for **Cu–(*S*)-17** and $\Delta F_D/\Delta F_L$ = 0.74 for **Cu–(*R*)-17**). Enantioselectivities with **Cu–(*S*)-17** for Phe and Trp are $\Delta F_D/\Delta F_L$ = 0.33 and $\Delta F_D/\Delta F_L$ = 0.63, respectively. **Cu–(*S*)-17** can be considered as an enantioselective fluorescence sensor for Pro in the concentration range analyzed (6×10^{-5}–6×10^{-4} M), used for the determination of the optical purity of proline in dilute solutions (6×10^{-4} M, 0.1 mg total amount).

Fluorescent monofunctionalized β-cyclodextrins (**18–23**) bearing a Cu^{2+} binding side arm and a dansyl group were designed as enantioselective sensors for unmodified α-amino acids (Fig. 10).[20] Enantioselectivity was evaluated by addition of Cu^{2+} complexes of D- or L-valine and D- or L-proline. The cyclodextrin **21** was found to be poorly enantioselective, as was similarly the case for **19**, suggesting that the best design can be obtained by using L-amino acids. All L-amino acid

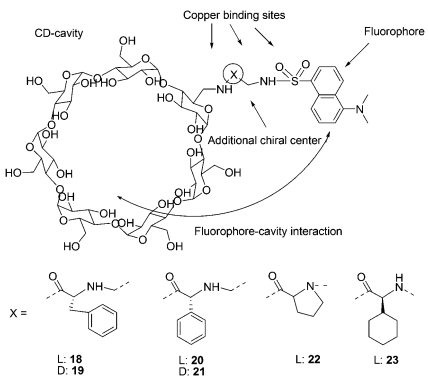

Fig. 10 Structures of cyclodextrins **18–23**, and structural elements considered in the design of enantioselective cyclodextrins.

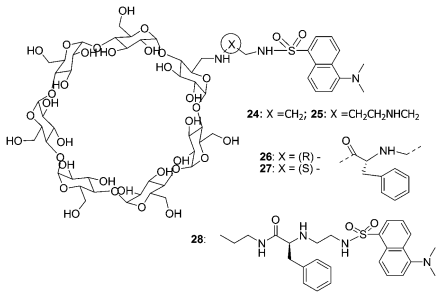

Fig. 11 Structures of cyclodextrins **24–28**, and structural elements considered in the design of enantioselective cyclodextrins.

containing cyclodextrins (**18**, **20**, **22**, **23**) showed good enantioselectivities. With **18** and **20**, enantiomers of α,α-disubstituted amino acids, *N*-methylamino acids, and amino acid amides were found to be discriminated.

In 2004, Corradini's group continued their work and discovered significant insights into the role of the cavity in the recognition process (Fig. 11).[21] Addition of D- or L-amino acids to the solution of **26** and **27** (0.1 M borate buffer pH = 7.3) induced increases in fluorescence intensity. With **26**, good enantioselectivity and high significance were found only in the case of Pro; Val and Ser gave significant differences at low amino acid excess, while Leu gave a significant difference only at 10 : 1 excess. When cyclodextrin **27** was used instead, the good enantioselectivities for Pro, Val, Leu, Ser, Phe, and PhGly at all ratios were obtained, while Lys and Tyr enantiomers were discriminated only at low molar excess values. The cyclodextrin **27** was more enantioselective than **26**, suggesting that the self-inclusion in the cyclodextrin cavity strongly increases the chiral discrimination ability of the Cu^{2+} complex.

2.1.2 Chemosensors based on zinc complexes. A molecular sensing ensemble with selectivity for aspartate was reported by Anslyn *et al.* (Fig. 12).[22] Pyrocatechol violet, **31**, was chosen for the displacement assay due to its ability to chelate the Zn^{2+} in **29** or **30**. The color changed from yellow (λ_{max} = 445 nm) to a deep blue (λ_{max} = 647 nm) upon addition of **29(OAc)$_2$** to a solution of the indicator in a water/methanol mixture (1 : 1; buffered with 10 mM HEPES at pH 7.4). Binding constants of 3.75×10^5 and 6.0×10^4 M^{-1} for 1 : 1 binding of **29** : **31** and **30** : **31** were obtained, respectively. The addition of various amino acids to an ensemble of **29** : **31** or **30** : **31** resulted in a color change from deep blue to yellow.

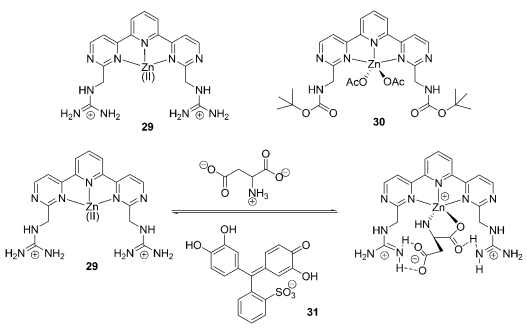

Fig. 12 Structures of **29** and **30**, and proposed binding mode of host **29**, indicator with amino acids.

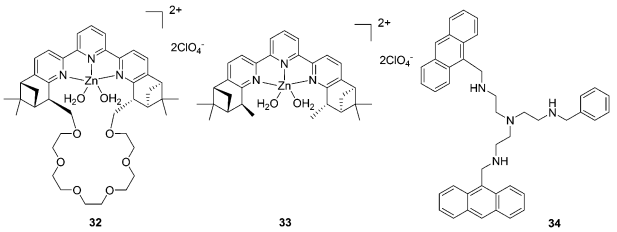

Fig. 13 Structures of compounds **32–34**.

The binding constants of **29** with hydrophobic amino acids such as glycine, valine, and phenylalanine were in the range of 1×10^4 M^{-1}.

A fluorescence macrocyclic receptor based on the Zn^{2+} complex of a C_2-terpyridine and a crown ether has been developed by Kwong and Lee *et al*. for molecular recognition of zwitterionic amino acids in water/DMF solution (Fig. 13).[23] Among the amino acids with a chelating group in the side-chain, L-aspartate (Asn) ($K = 4.5 \times 10^4$ M^{-1}, $\Delta G_0 = 26.5$ kJ mol^{-1}) and L-cysteine ($K = 2.5 \times 10^4$ M^{-1}, $\Delta G_0 = 25.1$ kJ mol^{-1}) showed the highest level of affinity towards receptor **32**. Receptor **33** also exhibited 1 : 1 binding towards L-aspartate with $K = 5 \times 10^2$ M^{-1}, which is about 90 times smaller than the K value of receptor **32**. This indicated that the Zn^{2+}-tpy and the crown ether are both essential for binding towards zwitterionic L-amino acids in water/DMF solutions. In the enantiomeric recognition studies, receptor **32** showed enantioselectivity towards the D-amino acids with $K_D/K_L = 3.0$.

The tetra-amino tripodal ligand, **34**, containing two anthracene subunits, has been prepared by Fabbrizzi and co-workers (Fig. 13).[24] The zinc complex, $\mathbf{[Zn^{2+}(34)]^{2+}}$, signals only the recognition of Trp through a drastic decrease of the fluorescent emission. The formation of a 1 : 1 receptor–amino acid adduct was proved, and the association constant log K was 4.21 ± 0.02 for Trp and 4.48 ± 0.05 for Phe. A π-stacking interaction involving the aromatic moieties positioned on the complex and on the amino acid induced extra stability of adducts with Trp (7 kJ mol^{-1}) and Phe (8 kJ mol^{-1}).

Rao *et al*. reported a lower-rim naphthylidene conjugate of calix[4]arene, **35** (**L**). **[ZnL]** could recognize aspartic acid (Asp), Cys, His, and Glu from among the naturally occurring amino acids by exhibiting large fluorescence quenching (Fig. 14).[25] The recognition features of **[ZnL]** toward amino acids seem to have bearing on protonation and chelating ability (His > Phe > Asp > Cys ≫ Glu), π–π interaction ability (Trp ≫ Tyr > His) of the side chain with the **[ZnL]**, and the dechelation of **[ZnL]** (His > Cys > Tyr > Asp ~ Trp). Extension of **[ZnL]** to proteins also resulted in dechelation of **[ZnL]** as well as aggregation of the protein with a trend: peanut agglutinin (PNA) < bovine serum albumin (BSA) < jacalin < human serum albumin (HSA).

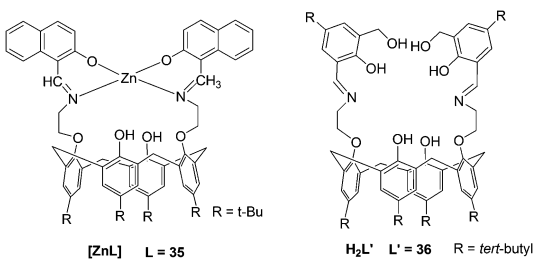

Fig. 14 The structures of the complexes.

A new 1,3-diderivative of calix[4]arene appended with hydroxymethyl salicylyl imine, **36** (**L′**), has been synthesized by Rao and co-workers (Fig. 14).[26] The receptor $\mathbf{H_2L'}$ showed selectivity toward Zn^{2+} through switch-on fluorescence with a detection limit of 192 ppb. The complex [**ZnL′**] was titrated with 20 naturally occurring amino acids which resulted in fluorescence quenching to different extents, and it follows a trend: Cys > Asp ≫ His.

2.1.3 Chemosensors based on other metal (Co, Pd, Rh) complexes. A plasticized polymer film, poly(vinyl chloride) (PVC), incorporated with a specific porphyrin dimer (**37**), is shown to exhibit significant and analytical usefulness for optical response toward His (Fig. 15).[27] With the optode membrane described, histidine in a sample solution from 0.0045 to 1.53 mM can be determined. The sensor presented exhibits high selectivity toward histidine over several amino acids in the following order: His ≫ Arginine (Arg) > Lys > Trp > isoleucine (Ile) > tyrosine (Tyr) > glycine (Gly) > Met. The high degree of histidine selectivity of the optode membrane makes it potentially useful for monitoring concentration levels of histidine in biological samples, such as human serum.

Xu *et al*. reported a cyclometalated palladium-azo complex, **38**, as a differential chromogenic probe for amino acids in aqueous solution at physiological pH (Fig. 16).[28] Amino acids with different side chain groups were clearly distinguishable in

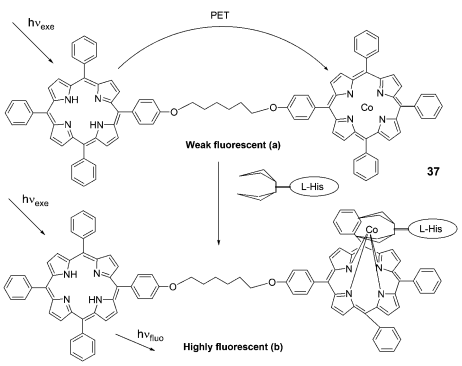

Fig. 15 Basic photoinduced electron-transfer process in a porphyrin dimer system: (a) in a free state and (b) guest-species-bound.

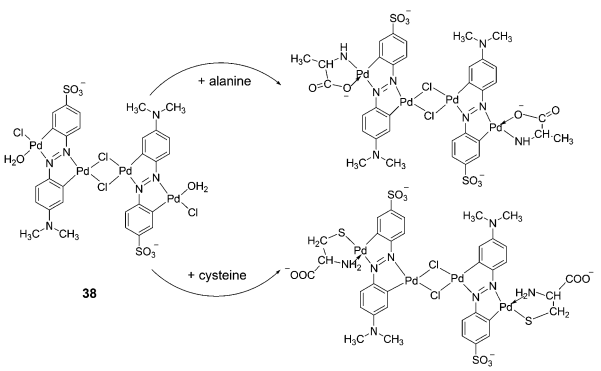

Fig. 16 Reaction of **38** with different α-amino acids.

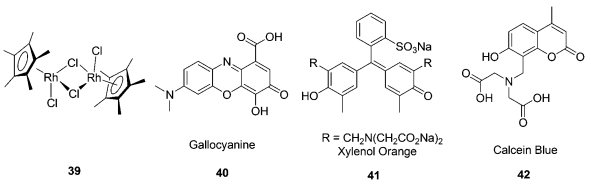

Fig. 17 The structures of Cp*Rh complex **39** and the dyes gallocyanine (**40**), xylenol orange (**41**), calcein (**42**).

their UV-Vis absorption spectra. For most of the amino acids, such as Cys, Met and Ala, the characteristic absorptions increased linearly with the concentrations of the amino acids titrated with the **38** sensing solutions over a concentration range 2.0×10^{-6}–10^{-5} M, without shifting the spectral shapes. However, in the case of Lys, λ_{max} shifted from 570 to 609 nm at a relatively higher concentration. The efficiency of the colorimetric response was also susceptible to the presence of coexisting inorganic ions.

Buryak and Severin reported a chemosensor array for the colorimetric identification of 20 natural amino acids (Fig. 17).[29] Organometallic Cp*Rh complex **39** was employed as the receptor unit for these IDAs. As the indicators, the dyes gallocyanine, xylenol orange, and calcein blue were employed. A key component of the sensor array was the utilization of a variable pH to change the selectivity of the IDAs. The UV/vis response at 750 nm of an IDA composed of **39** and **40** was used to classify the amino acids into a high-affinity (consisting of His, Cys, Met, Asp, Asn, $\Delta A(750\text{ nm}) < 0.06$) and a low-affinity (the remaining 15 amino acids ($0.55 > \Delta A(750\text{ nm}) > 0.06$) group. Each member of the first group was analyzed by four IDAs (by two different dyes, **41** and **42**, and at two different pH values), and each member of the second group was analyzed by five IDAs (by indicator **40**, at five different pH values). The sole cyclic amino acid, proline, and the closely related analytes such as leucine and isoleucine, are clearly distinguishable.

2.2 Reaction based chemosensors

2.2.1 Based on imine formation. Detection of amines and unprotected amino acids under aqueous conditions by formation of highly fluorescent iminium ions was reported by Feuster and Glass (Fig. 18).[30] The coumarin derivatives **43** and **44** were examined for their interactions with amino acids using UV/vis spectroscopy under high salt aqueous conditions (100 mM NaCl, 50 mM HEPES, pH = 7.4). Upon the addition of glycine, the equilibrium formation of the iminium ion was poor for **43** ($K_{eq} < 1$). In contrast, formation of the iminium ion was substantially more favorable for **44** ($K_{eq} = 4.0$) and was accompanied by a much larger (34 nm) red shift in absorption. Results indicated that all primary

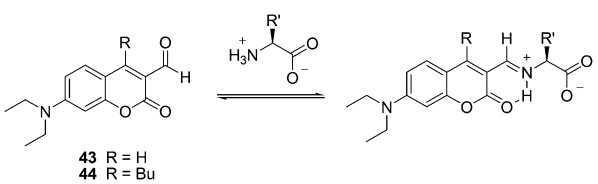

Fig. 18 The reaction mechanism of **43**, **44** with amino acids.

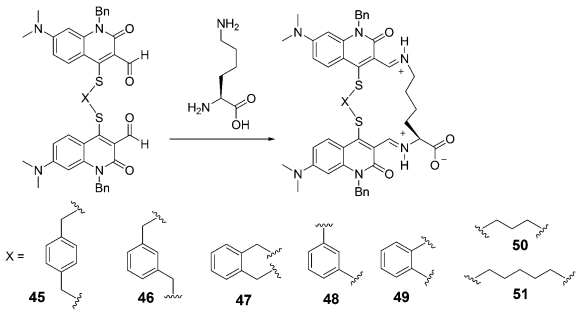

Fig. 19 The reaction mechanism of **45–51** with lysine.

amines give strong fluorescence responses with **44**, and secondary amines as well as hydroxy acids did not interact with sensor **44**. Upon titration with glycine, the fluorescence intensity of **44** at 513 nm increased 26-fold.

In 2005, Glass *et al*. reported sensors for diamines prepared by dimerization of a quinolone aldehyde core (Fig. 19).[31] The dimeric sensors bound the diamine guests by formation of a bis-iminium ion which produced large changes in the fluorescence of the quinolone core. In all cases, the diamines (lysine, ornithine, *etc*.) bound better than butylamine in 50% MeOH-buffered water (50 mM HEPES, 240 mM NaCl, pH = 7.4). The extent of the difference varied from 2.5 fold for sensor **45** to 160 fold for **51**. The maximum fluorescence change for **48** was much larger for ornithine ($K_a = 3300\ M^{-1}$) than for lysine ($K_a = 2100\ M^{-1}$) which may indicate a better binding geometry for ornithine. With respect to **51**, the bonds for lysine ($K_a = 2800\ M^{-1}$) and ornithine ($K_a = 2400\ M^{-1}$) are similar.

Yoon and Lee *et al*. reported a selective colorimetric and fluorescent chemosensor based on pyrene for lysine (Fig. 20).[32] A unique colorimetric change of **52** (CH_3CN–HEPES buffer, 0.01 M, pH 7.4, 1 : 9, v/v) from light yellow to pink takes place only in the presence of lysine. This induced color change can be easily observed by the naked eye. A dissociation constant for the complex formed between **52** and Lys was calculated to be $K_d = 2.78 \times 10^{-3}$ M from a linear plot of UV absorbance associated with 1 : 1 host–guest binding. In addition, a selective fluorescence enhancement occurs when **52** reacts with lysine and not with the other tested amino acids. The calculations revealed that the observed colorimetric change is a consequence of formation of a stacked dimeric form of the products in which an intramolecular H-bond interaction exists between the C=N and OH groups that is mediated by an H-bond water relay between the OH and lysine COOH groups.

2.2.2 Based on Michael addition. A regenerative, molecular machine-like "on–off–on" chemosensor based on a chromene molecule with the pyran ring "off–on–off" cycle was reported

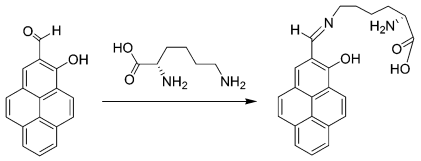

Fig. 20 The reaction mechanism of **52** with lysine.

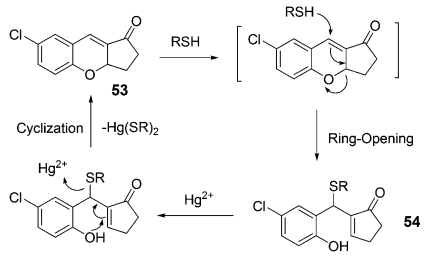

Fig. 21 The mechanism for the reaction of **53**.

by Yin *et al.* (Fig. 21).[33] It behaves as a molecular lock that requires a thiol "key" to open the lock and a mercury ion "hand" that unlatches the key for unsheathing the key to close the lock. It was indicated that probe **53** can respond to thiol at a low micromolar level, and a linear response of probe **53** to increasing amounts of even low Cys concentrations from 3×10^{-7} to 3.9×10^{-6} M was observed. Compound **54** may act as a fluorogenic chemosensor for the Hg^{2+} ions with high selectivity and sensitivity, and the detection limit for Hg^{2+} in aqueous buffer is at a low micromolar level, *e.g.*, 0.15–9.0 μM.

Kim and co-workers demonstrated a fluorescent probe **55** for biothiols (Cys, Hcy, GSH) (Fig. 22).[34] **55** exhibits a sensitive and selective fluorescence enhancement toward the biothiols over other natural amino acids, which is attributable to the Michael addition of a thiol group to the α,β-unsaturated malonitrile unit of **55**. In an aqueous solvent of **55** (DMSO/HEPES = 1 : 2, v/v, 0.1 M HEPES, pH 7.4), Cys has shown a dramatic increase (F/F_o = 19) in the fluorescence intensity over other natural amino acids. Hcy and GSH enhance the fluorescence intensity of **1** (F_o) by F/F_o 12- and 5.6-fold, respectively. Probe **55** was further applied for the cellular expression and the detection of biothiols in HeLa cells.

Yoon and Shin *et al.* developed a new fluorescein-based fluorescent probe for the detection of thiol-containing molecules (Fig. 23).[35] The probe **56** displayed fluorescence enhancements (λ_{max} = 520 nm) and UV-Vis spectral changes, which were attributed to 1,4-addition of thiols to α,β-unsaturated ketone in the probe to form thioether, in the presence of

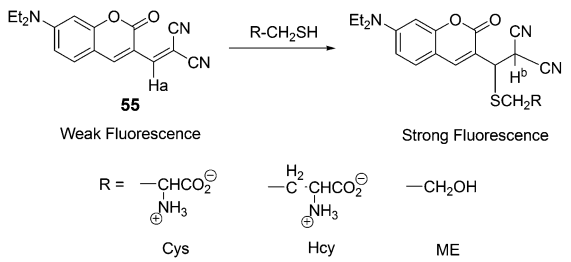

Fig. 22 Probe **55** and its thiol conjugates.

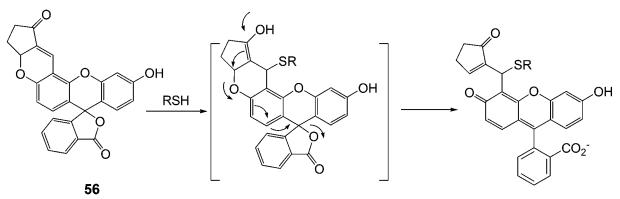

Fig. 23 A plausible mechanism of **56** to thiols in aqueous solution.

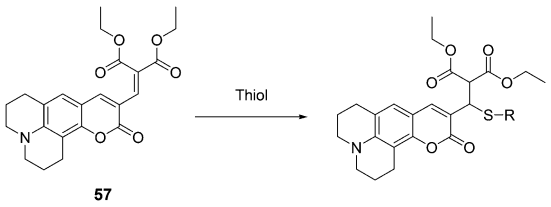

Fig. 24 The mechanism for the reaction of **57**.

thiol-containing analytes (Cys, homocysteine (Hcy) and glutathione (GSH)) in HEPES buffer (20 mM, pH 7.4, 1% CH_3CN). **56** also showed high sensitivity towards thiols with a detection limit of 10^{-7}–10^{-8} M, and the observed rate constants (k_{obs}) at pH 7.4 were found to be 36.5, 8.0 and 11.5 min^{-1} for Cys, Hcy and GSH, respectively.

Kim, Lee and Kang *et al.* reported a new coumarin-based chemodosimeter **57**, which could effectively and selectively recognize thiols based on a Michael type reaction, showing a preference for cysteine over other biological materials including homocysteine and glutathione (Fig. 24).[36] In aqueous solution (PBS buffer, pH 7.4, 10% DMSO), the fluorescence intensity is proportional to the amount of Cys added at the submicromolar level, with a coefficient of R = 0.99557 and a detection limit of 30 nM. The pK_a of Cys (8.30) is lower than that of Hcy (8.87) or GSH (9.20). The cysteine preference of **57** over homocysteine and glutathione was also demonstrated by LC-MS spectroscopic methods using the metabolite from the HepG2 cell line.

2.2.3 Based on formation of thiazinane or thiazolidine. A method for the selective fluorescence sensing of Hcy and Cys under neutral pH conditions was reported by Shao and Guo *et al.* (Fig. 25).[37] In a 0.1 M HEPES buffer of pH 7.4/CH_3CN (v/v, 2 : 3), the reaction of Hcy or Cys with probe **58** resulted in a significant fluorescence enhancement around 513 nm. The fluorescence quantum yields of **58** increased from 0.26 to 0.71 with Hcy, and from 0.26 to 0.63 with Cys. The binding constants for probe **58** with Hcy and Cys were determined to be 1300 M^{-1} and 741 M^{-1}, respectively. Surprisingly, no significant changes were observed in the fluorescence emission spectra and absorption spectra of **59** in the presence of Hcy or Cys. Therefore, it was demonstrated that the location of the aldehyde group at the Bodipy core is important and has an effect on the cyclization with Hcy/Cys.

A unique ruthenium(II) complex, **60**, has been reported by Yuan and Ye *et al.* as a luminescence probe for the recognition and detection of Cys and Hcy (Fig. 26).[38] The nearly non-luminescent probe can rapidly react with Cys and Hcy to yield

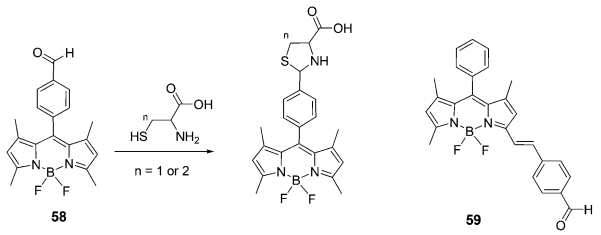

Fig. 25 Structures of **58**, **59** and the reaction of compound **58** with Hcy or Cys to form thiazinane (n = 2) or thiazolidine (n = 1).

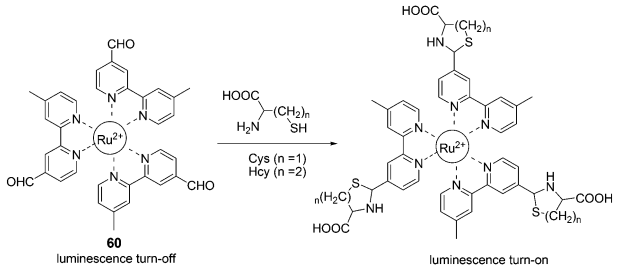

Fig. 26 The mechanism for the reaction for **60** and Hcy/Cys.

the corresponding thiazolidine and thiazinane derivatives, accompanied by the remarkable luminescence enhancement and a large blue-shift of the maximum emission wavelength from 720 to 635 nm. The dose-dependent luminescence enhancement of the probe shows a good linearity in the Cys/Hcy concentration range of 15 to 180 μM with detection limits of 1.41 μM and 1.19 μM for Cys and Hcy, respectively. The luminescence response of the probe is highly specific to Cys/Hcy even in the presence of various amino acids, protein, and DNA.

61, with efficient intramolecular charge transfer, was reported by Peng and Fan *et al.* as a fluorescent chemodosimeter for Cys and Hcy (Fig. 27).[39] Upon addition of Cys/Hcy, **61** exhibited greatly enhanced fluorescence intensity in acetonitrile–HEPES buffer (20 mM, pH = 7.4) solution (3 : 7, v/v). The fluorescence intensities of **61** at 560 nm showed a good linear relationship with the concentration of Cys, using physiological levels ranging from 0 to 500 mM. Its detection limit for Cys is 6.8×10^{-7} M in acetonitrile–HEPES. A large absorption peak shift of 70 nm (from 430 nm to 500 nm) appeared with a distinct isosbestic point at 452 nm, corresponding to an apparent color change from orange to yellow.

2.2.4 Based on cleavage of a sulfonate ester. A novel fluorescent probe was reported by Li and Ma *et al.* for the determination of cysteine in biological samples by incorporating the 2,4-dinitrobenzenesulfonyl (DBS) group as a quencher into the BODIPY skeleton (Fig. 28).[40] Upon reacting with cysteine, the probe produced a rapid and large fluorescence enhancement through the removal of the DBS unit by nucleophilic aromatic substitution. The fluorescence enhancement value was directly proportional to the concentration of cysteine (HEPES buffer (pH = 7.8) containing 50% (v/v) DMSO) in the range 2–12 μM, with a detection limit of 30 nM (S/N = 3). The applicability of the developed method has been successfully demonstrated on the determination of non-protein cysteine in human serum.

A styryl boron-dipyrromethene (BODIPY)/2,4-dinitrobenzenesulfonyl (DNBS) dyad based red-emitting molecular

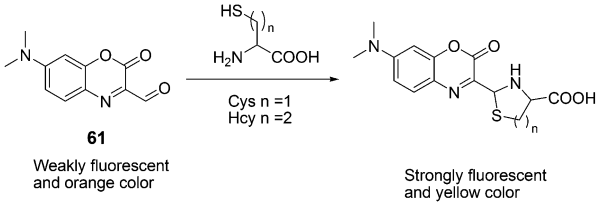

Fig. 27 Mechanism for the reaction of **61**.

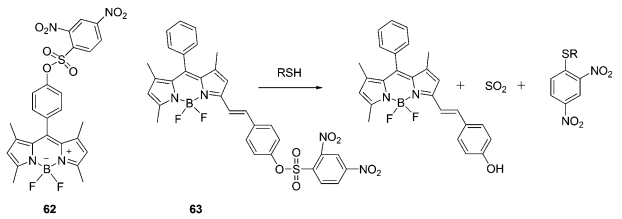

Fig. 28 Structures of **62**, **63** and the mechanism for the reaction of **63**.

probe for specific detection of cysteine among the biological thiols was reported by Zhao's group (Fig. 28).[41] This probe showed intensive absorption at 556 nm and the probe was non-fluorescent. The DNBS moiety can be cleaved off by thiols, the red emission of the BODIPY fluorophore at 590 nm was switched on, with an emission enhancement of 46-fold in a mixed solvent of MeOH/H_2O (4 : 1, v/v). The probe showed good specificity toward cysteine over other biological molecules, and the detection limit of probe **63** for cysteine was determined to be 7.2×10^{-6} M. The emission of the probe is pH-independent in the physiological pH range. The probe was used for fluorescent imaging of cellular thiols in SGC-H446 cells.

2.2.5 Based on cleavage of disulfide by thiols. A naphthalimide-based colorimetric fluorescent probe containing a disulfide group was reported by Wang and Zhang *et al.* (Fig. 29).[42] In a mixture of ethanol and water (1 : 9, v/v) solution containing phosphate buffered saline (PBS) (20 mM, pH 7.4), when GSH was added to the solution of **64**, the maximum absorption peak showed an 85 nm red shift and the colour of the solution turned from colourless to jade-green. Thus it can serve as a "naked-eye" probe for thiols. The maximum emission peak undergoes a red-shift of 48 nm, and the ratio of fluorescence intensities (F_{533}/F_{485}) (λ_{ex} = 400 nm) changes from 0.5 to 5.7 (R = 11.4-fold). A good linearity between the fluorescence intensity ratio, R (F_{533}/F_{485}) and the concentrations of GSH in the range of 0.5 to 10 mM with a detection limit of 28 μM was observed. The living cell image experiments further demonstrate the potential utility of **64** for the determination of thiols in living systems.

2.2.6 Based on metal complexes-displace coordination. A sensitive colorimetric sensor **65** toward α-amino acids was explored by Li and Zhang *et al.* (Fig. 30).[43] Upon the addition of copper ions, the original colorless solution of compound **65** became pink rapidly and the absorption peak at 555 nm clearly increased. In tris-HCl (10 mM, pH = 7.0) buffer containing 50% (v/v) water/CH_3CN, it was shown that the

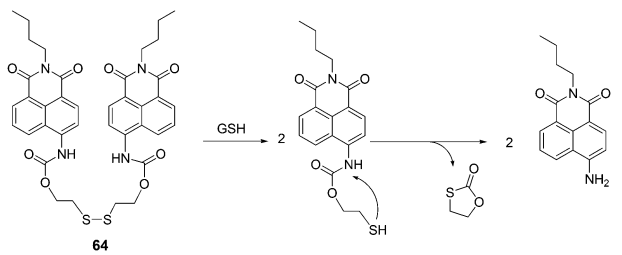

Fig. 29 Reaction mechanism of **64** and GSH.

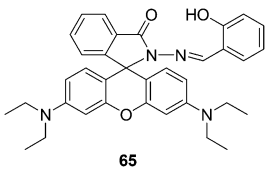

Fig. 30 Structure of compound **65**.

complex of **65** and copper ions could give a quick response to all these α-amino acids, especially toward His at the concentration of His as low as 1.3×10^{-5} mol L^{-1}. As the hydrolysis of bovine serum albumin (BSA) with the aid of trypsin produces α-amino acids, the complex **65**/Cu^{2+}/BSA could act as a label-free, selective sensor toward trypsin over the enzyme concentration from 0 to 5.0 μg mL^{-1}. The hydrolysis process of BSA in the presence of trypsin was visually observed by the naked eyes.

The combination of a new squaraine **66** and varied concentrations of Hg^{2+} was utilized to probe thiol-containing amino acids in an absorption or fluorescence turn-on manner (Fig. 31).[44] The formed complex between **66** and Hg^{2+} was consistent with a 1 : 1 binding mode, and the association constant was calculated to be 5.7×10^4 M^{-1}. Cysteine, homocysteine, glutathione, and histidine can completely restore the visible absorption and emission of **66** during the titration of acetonitrile/water (2 : 1) solutions of **66** (1 mM) and Hg^{2+} (20 mM). The absorption change from colorless to green was easily discernible by the naked eye.

Jiang and co-workers found that Hg^{2+} highly selectively bound to **67** that bears an imide group similar to that of thymine and specifically induced aggregation of **67** that led to a dramatic quenching of **67** fluorescence at 532 nm, thereby allowing for a sensitive and selective Hg^{2+} sensing and affording a non-fluorescent chemosensing ensemble "**67**–Hg" for thiol-containing species (Fig. 32).[45] Addition of thiol-containing amino acids to the Hg^{2+}–**67** ensemble solution (9 : 1 DMF–H_2O (v/v)) induced dissociation of the aggregates and recovery of the fluorescence. For Cys, a detection limit of 9.6 nM was obtained with a linear response over [Cys] of 0.05–0.3 μM.

2.2.7 Based on other approaches. Tae *et al.* reported a complex of Au^+ and a rhodamine hydroxylamine having 2-deoxyribose to detect cysteine and homocysteine in water (Fig. 33).[46] In the presence of Au^+, only Cys and Hcy experience dramatic enhancements in fluorescence intensities of **68**. As shown in Fig. 35, the recognition of Cys could be attributed to the binding of the thiol of Cys to the Au^+-bound

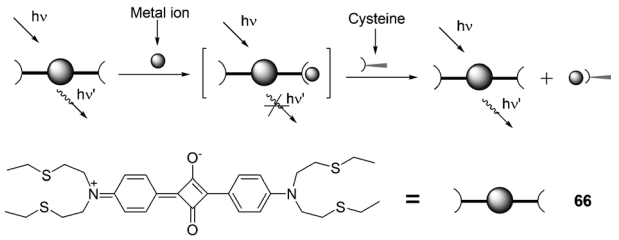

Fig. 31 Chemical structure of **66** and pictorial demonstration of its sensing of thiol-containing amino acids.

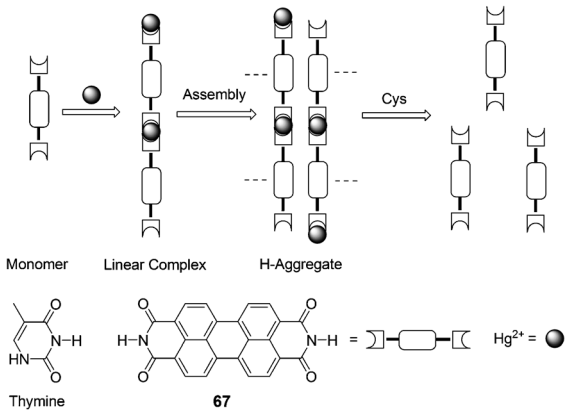

Fig. 32 Scheme of Hg^{2+} induced aggregation of **67** and aggregate dissociation in the presence of cysteine.

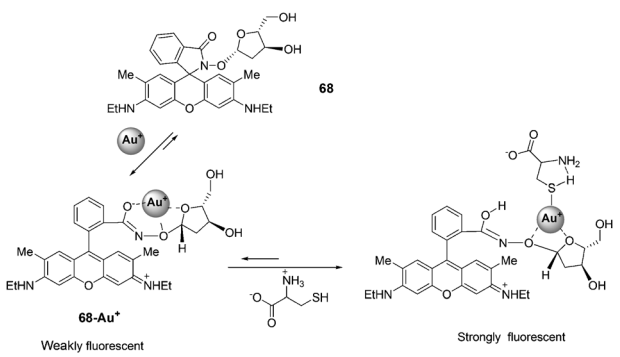

Fig. 33 Reaction of compound **68** with Cys.

probe. The binding stoichiometry of **68**–Au^+ with Cys was proved to be 1 : 1. The corresponding binding constant in H_2O (MeOH 1%) is $K_a = 6.65 \times 10^3$ M^{-1} and the detection of Cys is possible at the 100 nM level. The colorless to red color change ($\log \varepsilon^{530\ nm} = 4.512$ M^{-1} cm^{-1}) associated with the binding of **68**–Au^+ with Cys was detected visually. Other amino acids exhibited no color changes with **68**–Au^+ under the same conditions.

Lin *et al.* designed a native chemical ligation (NCL)-based ratiometric fluorescent thiol probe (**69**) for ratiometric imaging of thiols in living cells (Fig. 34).[47] The intramolecular energy transfer efficiency from the Bodipy donor to the rhodamine acceptor in **69** was calculated to be 98.4%. When **69** was titrated with increasing concentrations of Cys in potassium phosphate buffer (pH 7.4, containing 45% CH_3CN as a co-solvent), the intensity at 590 nm gradually decreased with the concomitant growth of a new emission peak at 510 nm, indicating that the FRET is off. The fluorescent intensity ratios at 510 and 590 nm (I_{510}/I_{590}) exhibited a drastic change from 0.09 to 24.82 with a 275-fold enhancement in the emission ratios. The detection limit of the probe was determined to be 8.2×10^{-8} M. **69** was then applied for thiol detection in real biological samples of serum, and for ratiometric imaging in living HeLa cells.

Che and Wong *et al.* developed FRET-based iridium(III) complexes for the detection of Hcy and Cys on the basis of conjugate addition of thiols to the vinyl sulfide linkage followed by elimination (Fig. 35).[48] In pH = 8.1 PBS

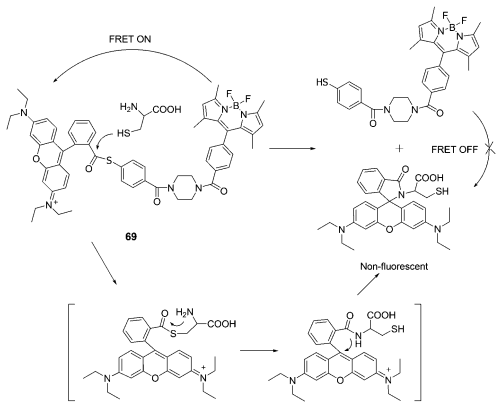

Fig. 34 Ratiometric fluorescent thiol probe **69** based on the NCL reaction.

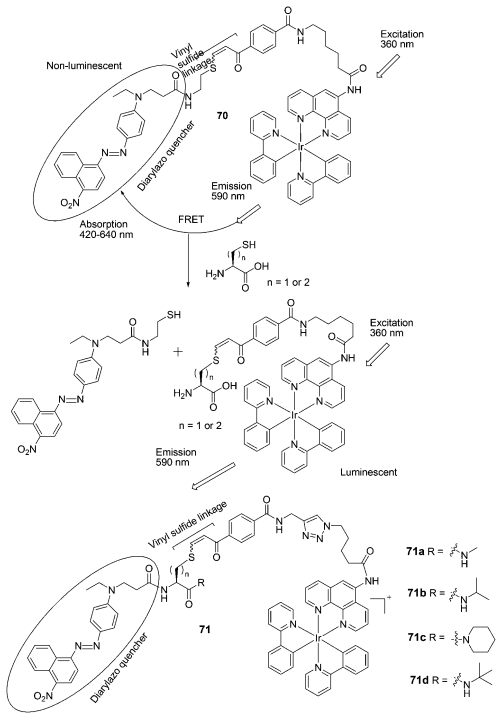

Fig. 35 Structures of **70**, **71a–71d** and the mechanism for the reaction for **70** and Hcy/Cys.

buffer/CH_3CN (1/3), the probes feature high selectivity for Hcy and Cys over other amino acids and GSH under physiological conditions. For **70**, the ratio of emission intensity enhancements upon the addition of Hcy and Cys is 1.4 : 1. The iridium(III) probe **71d** is able to differentiate Hcy from Cys in a ratio of 5 : 1. In addition, **71d** could be used for the detection of Hcy and Cys in human blood plasma.

2.3 Chemosensors utilizing hydrogen-bonds and π–π interaction

2.3.1 Chemosensors bearing thiourea binding sites. The binding affinities of a cholic-acid-based fluorescent neutral receptor toward dicarboxylate anions and amino acids have been investigated in a CH_3OH/H_2O system (1 : 1, 0.01 M HEPES buffer, pH = 7.4) by Chan's group (Fig. 36).[49] When treated with L-aspartate, glutamate, *N*-acetyl-L-aspartate and *N*-acetyl-L-glutamate, the emission spectrum of **72** can be quenched by *ca.* 20%. On the basis of the change of fluorescent intensity, the complex association constants (K_a) were calculated using nonlinear least-squares curve fitting. It revealed that the preorganization of **72** permits three points binding with the guests leading to a more selective complexation with acidic amino acids than their corresponding dicarboxylates, and **72** strongly binds glutamate *via* multiple hydrogen bonds with a binding constant of $(5.57 \pm 0.88) \times 10^6\ M^{-1}$.

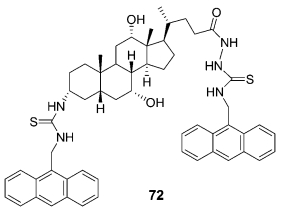

Fig. 36 Structure of **72**.

Chan and co-workers further reported that the chiral fluorescent probes **73** and **74** demonstrated differential binding toward trifunctional amino moieties (Fig. 37).[50] The emission spectrum of **73** was quenched by as much as 80% with the addition of 10 equivalents of D-serine, and the binding interaction of **73** to serine (D-serine $K_a = (2.26 \pm 0.17) \times 10^5\ M^{-1}$) is slightly stronger than that of **73** to threonine (D-threonine $K_a = (1.82 \pm 0.14) \times 10^5\ M^{-1}$), lysine (D-lysine $K_a = (1.37 \pm 0.11) \times 10^5\ M^{-1}$) and tyrosine (D-tyrosine $K_a = (1.94 \pm 0.09) \times 10^5\ M^{-1}$). Among the four pairs of enantiomeric amino acids, **73** showed a consistent bias for the D-amino acids with high K_D/K_L values from 6.7 to 8.9. In contrast to host **73**, opposite enantioselectivity toward serine, threonine, lysine and tyrosine was displayed by host **74** with high K_L/K_D values from 6.2 to 8.1. This implies that the chiral discrimination power of hosts **73** and **74** may be due to the 1,2-diaminocyclohexane moiety.

Two new anthracene thiourea derivatives, **75** and **76**, were investigated as fluorescent chemosensors for the chiral recognition of amino acids (Fig. 38).[51] The association constants of **75** with D- and L-*t*-Boc alanine were calculated as 11 800 and 2160 M^{-1}, respectively, and K_D/K_L was found to be 5.5. The association constants of **76** with D and L-*t*-Boc alanine were calculated as 2300 and 23 900 M^{-1}, respectively, and K_L/K_D

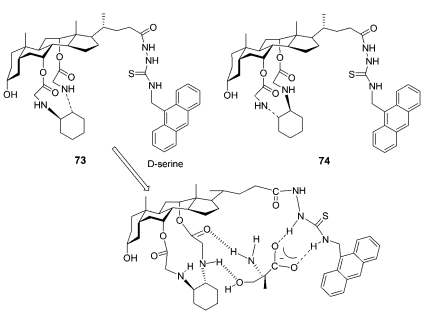

Fig. 37 Structures of fluorescent sensors **73**, **74** and the proposed binding mode of host **73** with D-serine.

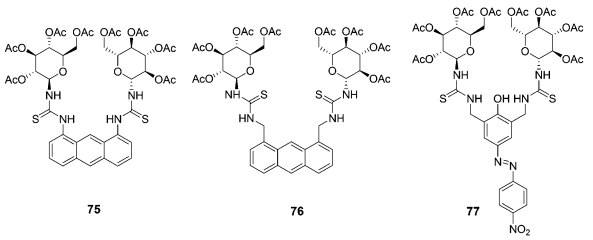

Fig. 38 Structures of **75**, **76** and **77**.

was found to be 10.4. These intriguing opposite D/L binding affinities for **75** and **76** were obtained without (or with) H–π interaction between the anthracene moiety and the methyl groups, which was explained by extensive high-level theoretical investigations taking into account the dispersion energy.

A new colorimetric anion sensor **77** was reported for chiral recognition (Fig. 38).[52] According to the linear Benesi–Hilderand expression, the measured absorption [**77**/($A - A_0$)] at 523 nm varied as a function of amino acids in linear relationship ($R \approx 0.9995$), indicating the 1 : 1 stoichiometry between amino acids and hosts. The association constants of **77** with L- and D-*t*-Boc threonine were calculated as 68 900 and 22 000 M^{-1}, respectively, and K_L/K_D was found to be 3.13. The D/L selectivity for alanine of host **77** was observed as high as 3.6, which was attributed to the glucopyranosyl unit (chiral barrier) of the host.

The anthracene based chiral fluorescent receptors **78** and **79** containing thiourea and amide groups were synthesized by He and co-workers (Fig. 39).[53] When the concentration of anions was gradually increased in DMSO, the fluorescence emission intensities of **78** at 429 nm decreased, while a new peak gradually enhanced at 538 nm. The solution color of **78** changed from light yellow to orange-red, which could be easily observed by the naked eye. Receptors **78** and **79** exhibited good enantioselective recognition towards the L-enantiomer of the chiral guests (L/D-malate, L/D-aspartate, and L/D-glutamate) with the $K_{ass(L)}/K_{ass(D)}$ values from 2.18 to 9.65.

The charge neutral chiral optical sensors **80–83** containing thiourea and amide groups were synthesized by He and co-workers (Fig. 39).[54] The different increasing efficiencies ($\Delta I_L/\Delta I_D = 1.8$) indicated that receptor **80** has a good enantioselective recognition ability between L- and D-α-Phe. In addition, the association constant (K_{ass}) of **80** with L-Phe is $(2.96 \pm 0.16) \times 10^4$ M^{-1}, while that of **80** with D-Phe is $(5.26 \pm 0.25) \times 10^3$ M^{-1}, and the enantioselectivity ($K_{ass(L)}/K_{ass(D)}$) is

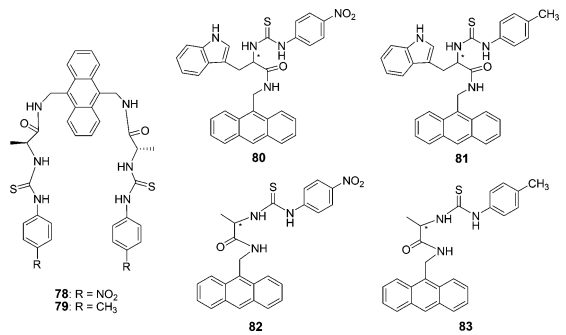

Fig. 39 Structures of **78–83**.

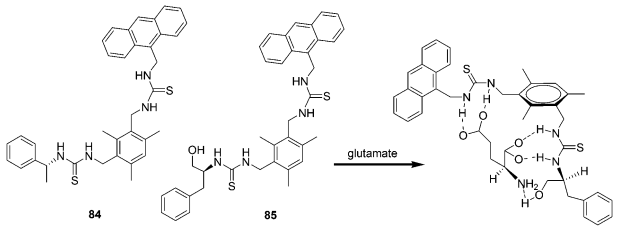

Fig. 40 Structures of fluorescent sensors **84**, **85** and the proposed binding mode of host **85** with glutamate.

5.63. On gradual increase of the concentration of L- and D-Phe, the intensity of the absorption band at 370 nm decreased, and a new absorption band appeared with a maximum absorption at 475 nm.

In 2011, Chan and co-workers continue their interest in this research direction and report two new sensing probes **84** and **85** (Fig. 40).[55] Operating on the PET mechanism, the fluorescent emission band of the host at 413 nm was quenched gradually upon the addition of the guest. As revealed by the respective association constants, sensor **84** showed the highest affinity to isophthalate ($K_a = (6.25 \pm 0.61) \times 10^4$ M^{-1}) in acetonitrile. The preorganization of sensor **85** permits three sites binding with the guests leading to enhanced complexation with aspartate and glutamate. The chiral recognition ability of the sensors is however, only moderate.

2.3.2 Chemosensors bearing other groups. Galactosyl-naphthyl-imine-based derivatives, **86** and **87**, were studied for their recognition of naturally occurring amino acids (Fig. 41).[56] The results thus indicate selective association between **87** and the four amino acids, Glu, His, Leu, and Pro, following a trend, namely, Leu > His > Pro based on the 455 nm fluorescence band and Leu ($K_a = 30911 \pm 700$) ≥ Glu ($K_a = 28733 \pm 3500$) ≫ His ≥ Pro based on the 355 nm fluorescence band. The slopes of these plots yielded a 1 : 1 complex for Leu, His, and Pro and a 2 : 1 complex for Glu. The titration of **86** with Ala, Cys, or Lys resulted in quenching of the fluorescence intensity. Both the changes of **86** in the fluorescence and absorbance followed an order: Lys ($K_a = 3162 \pm 300$) > Cys ($K_a = 1778 \pm 250$) > Ala.

A glucose based C2-glyco-conjugate (**88**) has been reported by Rao's group (Fig. 41).[57] Titration of **88** with all the 20 naturally occurring amino acids resulted in a large fluorescence intensity enhancement only in the case of aromatic amino acids, that is, Phe > Trp > His > Tyr. The association constants (K_a) were found to be 19 400 ± 600 for the aromatic amino acids. Two other non-aromatic amino acids, specifically alanine and arginine, exhibited K_a values of 3360 ± 225 and 1930 ± 150, respectively. Thus the aromatic amino acids combine with **88** by a factor of 5–10 times higher in affinity

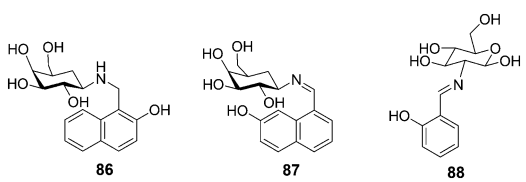

Fig. 41 Structures of **86**, **87** and **88**.

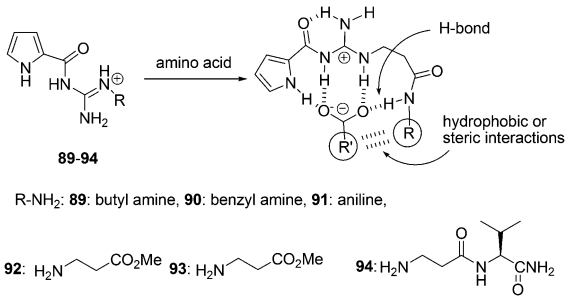

Fig. 42 Structures of sensors **89–94**, and the hydrophobic or steric interactions in their binding modes.

as compared to the non-aromatic ones. Therefore, **88** could recognize aromatic amino acids down to 1.5–3 ppm through switch-on fluorescence behavior.

N′-Substituted guanidiniocarbonyl pyrroles **89–94** were synthesized by Schmuck and Bickert as the efficient receptors for the complexation of amino acid even in water (bis-tris-buffer, 3 mM at pH = 6.1) (Fig. 42).[58] The addition of amino acid to a solution of **94** was tested using UV-titration studies. The absorbance of the pyrrole moiety at 290 nm decreased upon 1 : 1 association model complex formation. **94** strongly bound amino acid carboxylates in aqueous buffer solution with association constants of $K_{ass} \geq 10^3\ M^{-1}$. Furthermore, the complex stability seems to depend on the nature of the amino acid side chain. Valine is bound nearly two times better than alanine (K_{ass} = 1750 and 1000 M^{-1}, respectively).

Suzuki and co-workers reported receptors based on triaza-18-crown-6 ether combined with two guanidinium groups, which could bind amino acids in aqueous methanol solution (pH = 9.5) and showed fluorescence enhancement response by a PET (photoinduced electron transfer) mechanism (Fig. 43).[59] The absorption spectra of receptors **95–97** showed no changes upon the addition of guests or upon pH changes. Fluorescence spectra of receptors **95** and **96** showed little or no response towards amino acids except for lysine, which has a higher pK_a value (10.53) due to its alkyl ammonium terminal. The order of fluorescence enhancement factor (FE) values of **95** and **96** is *n*-BuNH_3^+ > lysine > GABA. In contrast, the order of FE values of receptor **97** is GABA > lysine > *n*-BuNH_3^+ > glycine.

The interaction and colorimetric sensing properties of the calix[4]pyrrole–TCBQ charge-transfer complex with amino acids and amines in $CHCl_3/EtOH/H_2O$ were investigated by Shao *et al.* (Fig. 44).[60] Upon the addition of lysine and arginine, the blue complex solution instantly turned orange-yellow. The CT absorption band at 612 nm nearly vanished, while a new absorption band appeared in the region of

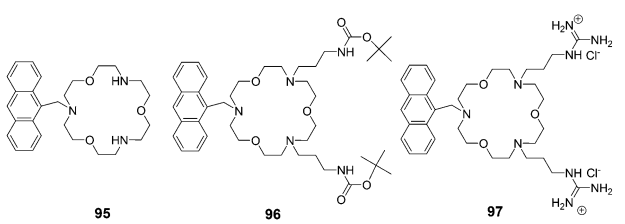

Fig. 43 Structures of sensors **95–97**.

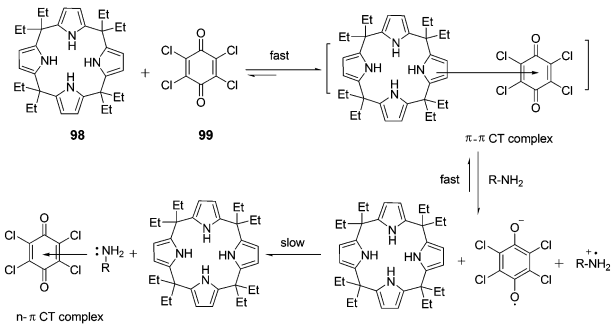

Fig. 44 The interaction mode of **98–99**.

400–500 nm. A similar, but less dramatic color change from blue to yellow-green was observed for histidine. The addition of aromatic amine and pyridine caused less significant changes in color and the CT absorption band at 612 nm, with the trend of aliphatic amines > pyridine > aromatic amine. Changes in color and absorption spectra of complex **98**·**99** in the presence of basic amino acids and aliphatic amines resulted from the disaggregation of the calix[4]pyrrole–TCBQ complex and the formation of a tetrachlorosemiquinone anion radical ($TCBQ^{\bullet -}$).

2.4 Chemosensors based on polymers

Compared to small organic compounds, polymer based optical sensors display several important advantages. Conjugated polymer chains with multiple recognition elements can increase both the binding efficiency and recognition selectivity for specific analytes. In addition, incorporating several different recognition units into a functional polymer can produce a valuable conclusion based on the combination of different outputs.[61]

In 2009, Li's group reported a disubstituted polyacetylene (**100**) which was utilized to sense α-amino acids over β- and γ-amino acids based on a 'turn-on' model (Fig. 45).[62] The strong blue fluorescence of **100** was quenched by trace copper ions efficiently, then the addition of α-amino acids to the **100**/Cu^{2+} complex in ethanol could recover the strong fluorescence of **100** to report the presence of α-amino acids. Among α-amino acids, the detection of His demonstrated even higher sensitivity with the detection limit lower than 1.3×10^{-5} M (2.1 ppm), and the fluorescent intensity of **100** was able to recover to about 88% at the concentration as low as 1.1×10^{-4} M. With the aid of a normal UV lamp, histidine could be visually differentiated from other α-amino acids by the

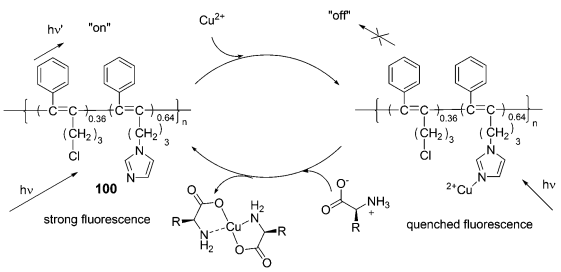

Fig. 45 The speculated conversion cycle of **100** in the presence of Cu^{2+} and α-amino acids.

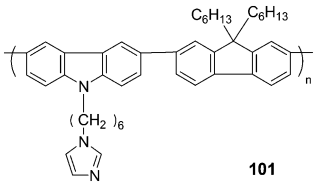

Fig. 46 The structure of **101**.

observation of its strong blue fluorescence, at concentrations as low as 4.0×10^{-5} M.

A conjugated fluorescent polymer was utilized to probe α-amino acids as shown by Li *et al.* (Fig. 46).[63] The strong fluorescence of the prepared polyfluorene (**101**) was quenched by trace copper ions. As Gly was added to the complex of **101** and copper ions, the quenched fluorescence of **101** turned on even at a concentration of Gly as low as 0.33×10^{-5} M (0.24 ppm). All of the α-amino acids could be detected sensitively, among them the detection of histidine (His) demonstrated highest sensitivity. The fluorescent intensity of **101** recovered to about 96% at a His concentration as low as 3.0×10^{-5} M. The reason that the detection sensitivity of His was higher than those of other α-amino acids was because the imidazole moieties in it may help His take the copper ions from the imidazole moieties in **101**.

Jiang's group developed a spectral signaling ensemble that is highly selective for and sensitive to Cys, which operates in a "mix-and-measure" mode. The formation of the coordination polymers is shown to be facilitated by both the Ag^+–Ag^+ interaction and the interaction between the side chains in the polymeric backbone. It shows that the electrostatic interaction among the Cys side chains plays an important role in maintaining the Ag^+–SR polymeric structure, and extended sensing systems can be constructed by manipulating the interactions among the –SR chains (Fig. 47).[64] With preliminary data on the corresponding Cu^+–Cys and Au^+–Cys systems that exhibited similar spectral signals, the M^+–SR coordination polymers (M = Au, Ag, or Cu) are assumed to be able to serve as spectral sensing platforms.

2.5 Chemosensors based on gold/silver nanoparticles

Patel and Menon reported *p*-sulfonatocalix[4]arene thiol modified gold nanoparticles as a colorimetric sensor to probe lysine, arginine and histidine in water (Fig. 48).[65] When 11 different aqueous solutions of amino acids in PBS buffer were added to calyx-capped gold nanoparticles, after half an hour, the solutions containing Lys, Arg or His had changed the color from red to purple with a red shift (524 nm to 550 nm region) and a broadening of the surface plasmon band which

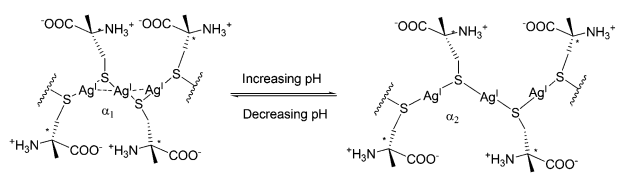

Fig. 47 Switching argentophilic attraction by the pH-modulated electrostatic interaction between adjacent ligands along the Ag(I)-Cys polymeric backbone. α_1 and α_2 are the Ag–S–Ag angles at low and high pH, respectively, $\alpha_1 < \alpha_2$.

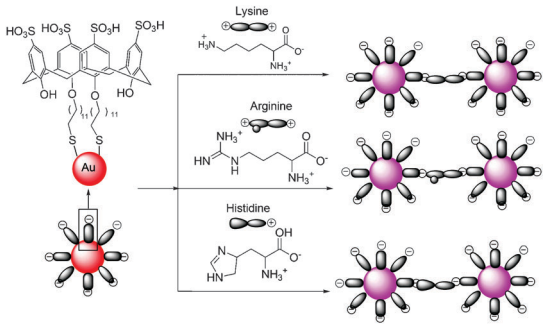

Fig. 48 A schematic representation of the amino acid induced aggregation of calix-capped gold nanoparticles.

was accompanied by aggregation of the nanoparticles. However after 24 h, the color disappeared very slowly due to sedimentation. A linear correlation existed between $A_{\lambda_{max}}$ and the logarithm of the Lys, Arg and His concentration C over the range of 10^{-6}–10^{-4} M, 4×10^{-6}–10^{-4} M and 2×10^{-6}–10^{-4} M with the linear detection limits of 1 μM, 4 μM and 2 μM, respectively.

Joo *et al.* reported that hydrogen bonding-induced redispersion of the aggregated Au nanoparticles upon *N*-hydroxysuccinimide ester bioconjugations could work as an optical sensor to detect a trace amount of amino acids as low as 10^{-6} M in an aqueous solution (Fig. 49).[66] The color of initially red pristine AuNPs became blue after modification with the DPAN group. The color returned to red upon conjugation with tyrosine in the concentration range of 10^{-6}–10^{-2} M within 2 h. Glycine, histidine, or tyrosine exhibited improved recovery behaviours than asparagines, glutamine, leucine, lysine, serine, and tryptophan under the present experimental conditions.

Yan *et al.* reported a resonance light scattering (RLS) bioassay for detecting Hcy in biological fluids based on Hcy-involved assembly of polyethyleneimine (PEI)-capped Ag-nanoclusters (Fig. 50).[67] It revealed that the increased RLS signal did not originate from the aggregation of the Ag-nanoclusters, rather from Hcy-involved assembling of PEI-capped Ag-nanoclusters. ΔRLS linearly increased with C_{Hcy} from 0.2 to 3.5 μM with a calibration function of

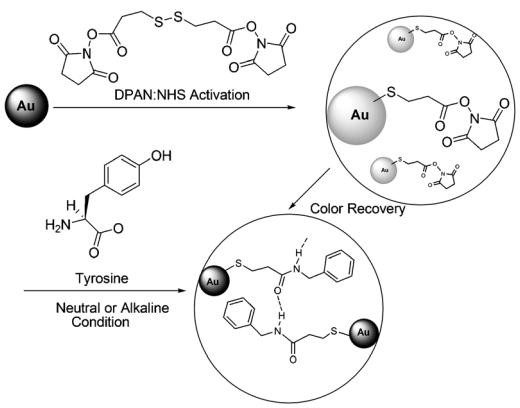

Fig. 49 Experimental scheme of NHS coupling of tyrosine and 3,3′-dithiopropionic acid di(NHS ester) (DPAN) adsorbed on Au nanoparticles.

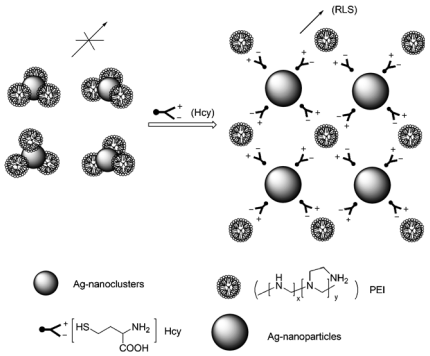

Fig. 50 Schematic illustration of Hcy-involved assembling of PEI-capped Ag-nanoclusters.

$\Delta RLS = 2346C_{Hcy} - 66$ (C_{Hcy} in μM, $R^2 = 0.9982$). The detection limit (S/N = 3) is 42 nM, and the precision for eleven replicate detections of Hcy at 1 μM is 0.6%, showing excellent reproducibility of the present bioassay. The bioassay allows discrimination of Hcy from Cys, GSH and other amino acids, and permits detecting trace Hcy in biological fluids (human serum samples).

2.6 Chemosensor arrays based on cucurbiturils supramolecular assembly

With the fluorescent dye Dapoxyl and the macrocyclic host cucurbit[7]uril (CB7, composed of 7 glycoluril units), a multi-parameter sensor array has been designed by Nau *et al.* (Fig. 51).[68] It showed the highly selective sensing of biomolecular analytes, either an amino acid (histidine, arginine, lysine, and tyrosine) or its corresponding decarboxylase. The detection can be transferred to a microtiter plate format with a limiting sensitivity of 2.4 nM per well. The extension of the high selectivity and μM sensitivity of the tandem assay principle has also allowed for the accurate measurement of D-lysine enantiomeric excesses of up to 99.98%.

A sensor array made by combining four fluorescent tricyclic basic dyes with cucurbiturils was reported by Baumes and Garcia *et al.* (Fig. 52).[69] This array was able to identify and discriminate 18 α-amino acids up to 10^{-4} M without the need of enzyme activation. The chemosensor array achieved a perfect cross-selectivity for AA, with a discrimination event (color change in fluorescence images), which was easily detected by the naked eye. It appeared that the discrimination between AA and the corresponding carboxylic acid is easier for PF and AO, while discrimination between a given AA and its corresponding amine is clearer for the OX dye. Pyronine (PYY) discriminates all three (AA, amine, and carboxylic acid derivative) in one shot.

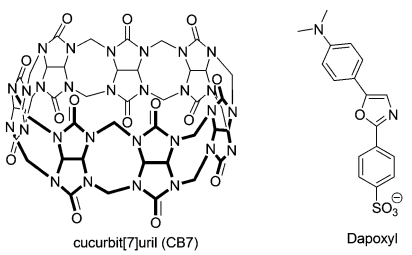

Fig. 51 Structures of cucurbi[7]uril and dapoxyl.

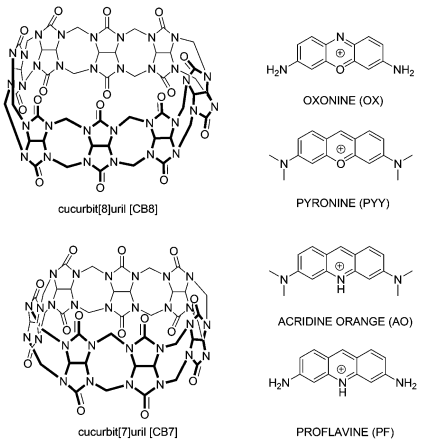

Fig. 52 Structures of cucurbi[7]uril, oxonine, pyronine, acridine orange and proflavine.

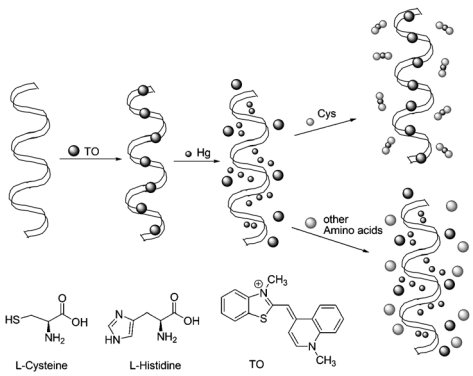

Fig. 53 Illustration of the TO/DNA/Metal ion-based amino acid sensor.

2.7 Chemosensors utilizing DNA

Ren's group reported a selective fluorescence turn-on assay for detection of cysteine and histidine using a DNA/ligand/ion ensemble (Fig. 53).[70] The high sensitivity and selectivity for cysteine and histidine were achieved by changing the metal ions (Hg^+ and Cu^{2+}). Upon the addition of cysteine to the solution of the TO/DNA/Hg^{2+} ensemble, the quenched fluorescence of TO/DNA turned on immediately. The enhanced fluorescence intensity is proportional to the cysteine concentration in the range from 2.5×10^{-9} to 1.1×10^{-7} M, and the detection limit of cysteine is 5.1×10^{-9} M. In the TO/DNA/Cu^{2+} system, both histidine and cysteine dislodged Cu^{2+} and restored the fluorescence of TO/DNA. The detection of histidine demonstrated even greater sensitivity than cysteine in this system. The detection limit was 1.0×10^{-8} M for histidine, and the linear range was from 0 to 4.4×10^{-6} M. Additionally, the detection and discrimination process can be detected with the naked eye under a hand-held UV lamp and may be easily adapted to automated high-throughput screening.

3. Concluding remarks

In this tutorial review we focused on the recent noteworthy reports regarding amino acid sensing since 2000. Depending on the significant characteristic properties of various amino

acids thus far, the optical probes utilizing indicator-displacement assays,[11–18,22,29] metal complexes coordination,[19–21,23–29,48] specific reactions between probes and amino acids[30–50] and other ways have been widely studied. For the reaction based probes, we further classified them into imine formation, Michael addition, thiazinane or thiazolidine formation, cleavage of a sulfonate ester, cleavage of disulfide, metal complexes-displace coordination and others. Due to the similarity in structure and reactivity of some amino acids, it is still challenging to develop sensors that can selectively and sensitively discriminate amino acids from one another, such as the three biological thiols Cys, Hcy and GSH.[35–39,46–48] This is not an easy task but the rapid progress documented so far has been encouraging and indicates that more successful probes differentiating various amino acids can be developed with fine tuning and careful design, especially intelligent combinations of basic organic reactions and communicating methods. Furthermore, sensing of various amino acids can be even possible by using receptor arrays composed of different chemosensors.[71] Finally, it is our hope that this tutorial review will inspire more chemists and biologists to explore novel and unconventional chemical scaffolds for the challenge of amino acid recognition and their applications in complex biological systems.

Acknowledgements

This research was supported by the Basic Science Research Program through the National Research Foundation of Korea (NRF) (2010-0018895) and by the Converging Research Center Program through the Ministry of Education, Science and Technology (2010K001202). The paper (YZ) was also supported by RP-grant 2010 of Ewha Womans University. YZ also acknowledges the Natural Science Foundation for the Youth (of China).

Notes and references

1 S. Shahrokhian, *Anal. Chem.*, 2001, **73**, 5972.
2 H. Yoshida, Y. Nakano, K. Koiso, H. Nohta, J. Ishida and M. Yamaguchi, *Anal. Sci.*, 2001, **17**, 107.
3 G. N. Chen, X. P. Wu, J. P. Duan and H. Q. Chen, *Talanta*, 1999, **49**, 319.
4 G. M. Mackay, C. M. Forrest, N. Stoy, J. Christofides, M. Egerton, T. W. Stone and L. G. Darlington, *Eur. J. Neurol.*, 2006, **13**, 30.
5 H. Refsum, P. M. Ueland, O. Nygård and S. E. Vollset, *Annu. Rev. Med.*, 1989, **49**, 31.
6 C. S. Lee, P. F. Teng, W. L. Wong, H. L. Kwong and A. S. C. Chan, *Tetrahedron*, 2005, **61**, 7924.
7 J. Wang, M. Chtrathi and B. Tian, *Anal. Chem.*, 2000, **72**, 5774.
8 D. Vardanega and C. Giradet, *Chem. Phys. Lett.*, 2009, **469**, 172.
9 Y. Zhou, Z. Xu and J. Yoon, *Chem. Soc. Rev.*, 2011, **40**, 2222.
10 X. Chen, Y. Zhou, X. Peng and J. Yoon, *Chem. Soc. Rev.*, 2010, **39**, 2120.
11 G. Klein and J.-L. Reymond, *Angew. Chem.*, 2001, **113**, 1821 (*Angew. Chem., Int. Ed.*, 2001, **40**, 1768).
12 K. E. S. Dean, G. Klein, O. Renaudet and J.-L. Reymond, *Bioorg. Med. Chem. Lett.*, 2003, **13**, 1653.
13 M. A. Hortalá, L. Fabbrizzi, N. Marcotte, F. Stomeo and A. Taglietti, *J. Am. Chem. Soc.*, 2003, **125**, 20.
14 M. Bonizzoni, L. Fabbrizzi, G. Piovani and A. Taglietti, *Tetrahedron*, 2004, **60**, 11159.
15 J. F. Folmer-Andersen, V. M. Lynch and E. V. Anslyn, *Chem.–Eur. J.*, 2005, **11**, 5319.
16 J. F. Folmer-Andersen, V. M. Lynch and E. V. Anslyn, *J. Am. Chem. Soc.*, 2005, **127**, 7986.
17 J. F. Folmer-Andersen, M. Kitamura and E. V. Anslyn, *J. Am. Chem. Soc.*, 2006, **128**, 5652.
18 D. Leung, J. F. Folmer-Andersen, V. M. Lynch and E. V. Anslyn, *J. Am. Chem. Soc.*, 2008, **130**, 12318.
19 S. Pagliari, R. Corradini, G. Galaverna, S. Sforza, A. Dossena and R. Marchelli, *Tetrahedron Lett.*, 2000, **41**, 3691.
20 R. Corradini, C. Paganuzzi, R. Marchelli, S. Pagliari, S. Sforza, A. Dossena, G. Galaverna and A. Duchateau, *Chirality*, 2003, **15**, 30.
21 S. Pagliari, R. Corradini, G. Galaverna, S. Sforza, A. Dossena, M. Montalti, L. Prodi, N. Zaccheroni and R. Marchelli, *Chem.–Eur. J.*, 2004, **10**, 2749.
22 H. Aït-Haddou, S. L. Wiskur, V. M. Lynch and E. V. Anslyn, *J. Am. Chem. Soc.*, 2001, **123**, 11296.
23 H.-L. Kwong, W.-L. Wong, C.-S. Lee, C.-T. Yeung and P.-F. Teng, *Inorg. Chem. Commun.*, 2009, **12**, 815.
24 L. Fabbrizzi, M. Licchelli, A. Perotti, A. Poggi, G. Rabaioli, D. Sacchi and A. Taglietti, *J. Chem. Soc., Perkin Trans. 2*, 2001, 2108.
25 P. C. Jugun, A. Acharya, A. Kumar and C. P. Rao, *J. Phys. Chem. B*, 2009, **113**, 12075.
26 R. Joseph, J. P. Chinta and C. P. Rao, *J. Org. Chem.*, 2010, **75**, 3387.
27 R. Yang, K. Wang, L. Long, D. Xiao, X. Yang and W. Tan, *Anal. Chem.*, 2002, **74**, 1088.
28 S.-H. Li, C.-W. Yu and J.-G. Xu, *Chem. Commun.*, 2005, 450.
29 A. Buryak and K. Severin, *J. Am. Chem. Soc.*, 2005, **127**, 3700.
30 E. K. Feuster and T. E. Glass, *J. Am. Chem. Soc.*, 2003, **125**, 16174.
31 K. Secor, J. Plante, C. Avetta and T. Glass, *J. Mater. Chem.*, 2005, **15**, 4073.
32 Y. Zhou, J. Won, J. Y. Lee and J. Yoon, *Chem. Commun.*, 2011, **47**, 1997.
33 F.-J. Huo, Y.-Q. Sun, J. Su, Y.-T. Yang, C.-X. Yin and J.-B. Chao, *Org. Lett.*, 2010, **12**, 4756.
34 H. Kwon, K. Lee and H.-J. Kim, *Chem. Commun.*, 2011, **47**, 1773.
35 X. Chen, S.-K. Ko, M. J. Kim, I. Shin and J. Yoon, *Chem. Commun.*, 2010, **46**, 2751.
36 H. S. Jung, K. C. Ko, G.-H. Kim, A.-R. Lee, Y.-C. Na, C. Kang, J. Y. Lee and J. S. Kim, *Org. Lett.*, 2011, **13**, 1498.
37 Y. Yue, Y. Guo, J. Xu and S. Shao, *New J. Chem.*, 2011, **35**, 61.
38 R. Zhang, X. Yu, Z. Ye, G. Wang, W. Zhang and J. Yuan, *Inorg. Chem.*, 2010, **49**, 7898.
39 M. Hu, J. Fan, H. Li, K. Song, S. Wang, G. Cheng and X. Peng, *Org. Biomol. Chem.*, 2011, **9**, 980.
40 J. Lu, C. Sun, W. Chen, H. Ma, W. Shi and X. Li, *Talanta*, 2011, **83**, 1050.
41 J. Shao, H. Guo, S. Ji and J. Zhao, *Biosens. Bioelectron.*, 2011, **26**, 3012.
42 B. Zhu, X. Zhang, Y. Li, P. Wang, H. Zhang and X. Zhuang, *Chem. Commun.*, 2010, **46**, 5710.
43 X. Lou, L. Zhang, J. Qin and Z. Li, *Langmuir*, 2010, **26**, 1566.
44 C. Luo, Q. Zhou, B. Zhang and X. Wang, *New J. Chem.*, 2011, **35**, 45.
45 Y.-B. Ruan, A.-F. Li, J.-S. Zhao, J.-S. Shen and Y.-B. Jiang, *Chem. Commun.*, 2010, **46**, 4938.
46 Y.-K. Yang, S. Shim and J. Tae, *Chem. Commun.*, 2010, **46**, 7766.
47 L. Long, W. Lin, B. Chen, W. Gao and L. Yuan, *Chem. Commun.*, 2011, **47**, 893.
48 H.-Y. Shiu, M.-K. Wong and C.-M. Che, *Chem. Commun.*, 2011, **47**, 4367.
49 S.-Y. Liu, L. Fang, Y.-B. He, W.-H. Chan, K.-T. Yeung, Y.-K. Cheng and R.-H. Yang, *Org. Lett.*, 2005, **7**, 5825.
50 H. Wang, W.-H. Chan and A. W. M. Lee, *Org. Biomol. Chem.*, 2008, **6**, 929.
51 Y. K. Kim, H. N. Lee, N. J. Singh, H. J. Choi, J. Y. Xue, K. S. Kim, J. Yoon and M. H. Hyun, *J. Org. Chem.*, 2008, **73**, 301.
52 M. K. Choi, H. N. Kim, H. J. Choi, J. Yoon and M. H. Hyun, *Tetrahedron Lett.*, 2008, **49**, 4522.
53 X.-H. Huang, Y.-B. He, Z.-H. Chen, C.-G. Hu and G.-Y. Qing, *Can. J. Chem.*, 2008, **86**, 170.
54 X.-H. Huang, Y.-B. He, C.-G. Hu and Z.-H. Chen, *J. Fluoresc.*, 2009, **19**, 97.

55 X. Zhou, Y. Yip, W. Chan and A. W. M. Lee, *Beilstein J. Org. Chem.*, 2011, **7**, 75.
56 R. Ahuja, N. K. Singhal, B. Ramanujam, M. Ravikumar and C. P. Rao, *J. Org. Chem.*, 2007, **72**, 3430.
57 A. Mitra, J. P. Chinta and C. P. Rao, *Tetrahedron Lett.*, 2010, **51**, 139.
58 C. Schmuck and V. Bickert, *Org. Lett.*, 2003, **5**, 4579.
59 S. Sasaki, A. Hashizume, D. Citterio, E. Fujii and K. Suzuki, *Tetrahedron Lett.*, 2002, **43**, 7243.
60 K. Liu, L. He, X. He, Y. Guo, S. Shao and S. Jiang, *Tetrahedron Lett.*, 2007, **48**, 4275.
61 H. N. Kim, Z. Guo, W. Zhu, J. Yoon and H. Tian, *Chem. Soc. Rev.*, 2011, **40**, 79.
62 Q. Zeng, L. Zhang, Z. Li, J. Qin and B. Z. Tang, *Polymer*, 2009, **50**, 434.
63 Z. Li, X. Lou, Z. Li and J. Qin, *ACS Appl. Mater. Interfaces*, 2009, **1**, 232.
64 J. Shen, D. Li, M. Zhang, J. Zhou, H. Zhang and Y. Jiang, *Langmuir*, 2011, **27**, 481.
65 G. Patel and S. Menon, *Chem. Commun.*, 2009, 3563.
66 J.-H. Park, E. O. Ganbold, D. Uuriintuya, K. Lee and S.-W. Joo, *Chem. Commun.*, 2009, 7354.
67 S.-K. Sun, H.-F. Wang and X.-P. Yan, *Chem. Commun.*, 2011, **47**, 3817.
68 D. M. Bailey, A. Hennig, V. D. Uzunova and W. M. Nau, *Chem.–Eur. J.*, 2008, **14**, 6069.
69 L. A. Baumes, M. Buaki, J. Jolly, A. Corma and H. Garcia, *Tetrahedron Lett.*, 2011, **52**, 1418.
70 F. Pu, Z. Huang, J. Ren and X. Qu, *Anal. Chem.*, 2010, **82**, 8211.
71 A. T. Wright and E. V. Anslyn, *Chem. Soc. Rev.*, 2006, **35**, 14.